Tribology International 70 (2014) 83–93

Contents lists available at ScienceDirect

Tribology International

journal homepage: www.elsevier.com/locate/triboint

Torque loss of type C40 FZG gears lubricated with wind turbine gear oils

Carlos M.C.G. Fernandes [a,*], Ramiro C. Martins [a], Jorge H.O. Seabra [b]

[a] INEGI, Universidade do Porto, Campus FEUP, Rua Dr. Roberto Frias 400, 4200-465 Porto, Portugal
[b] FEUP, Universidade do Porto, Rua Dr. Roberto Frias s/n, 4200-465 Porto, Portugal

ARTICLE INFO

Article history:
Received 23 July 2013
Received in revised form
27 September 2013
Accepted 5 October 2013
Available online 12 October 2013

Keywords:
Wind turbine gear oils
Rolling bearings
Gears
Efficiency

ABSTRACT

Five fully formulated wind turbine gear oils were characterised. The gear oils have 320 ISO VG grade and different formulations: ester, mineral, PAO, PAG and mineral+PAMA.

A back-to-back FZG test machine, with re-circulating power, was used and a torque-cell was included on the test rig in order to measure the torque loss. Eight thermocouples were included to monitor the temperatures in different locations of the test rig.

Tests at 1.13, 2.26 and 6.79 m/s were performed for different FZG load stages: K1, K5, K7 and K9. Both gearboxes were jet-lubricated with an oil flow of 3 l/min. The input flow temperature was kept almost constant (80 ± 1 °C).

Friction generated between the meshing teeth, shaft seals and rolling bearing losses was predicted.

1. Introduction

The generation of electricity by wind power is becoming more popular due to the concerns about the effects of global warming [1,2]. To make wind energy competitive with other power plants in the near future, enhancements on availability, reliability and lifetime will be required. The isolated locations where the plants are built, and the complex forces which interact in unexpected and damaging ways, have led to high failure rates for various different components in the turbine, with the gearbox being the most problematic. Combined with the high repair costs, the downtime due to gearbox failure is usually far greater than any other component failures. This leads to higher operational costs and it has become a plague for wind power industry [3–6]. These situations had led to new solutions like direct drive wind turbines which do not necessarily have better reliability than geared drive turbines [7].

Wind turbine gearbox problems can start with the oil. According to DIN recommendations the best viscosity and anti-scuffing properties are reached for oil operating temperatures above 80 °C. In wind turbine gearboxes where temperatures do not exceed 60 °C the anti-scuffing class tends to drop, resulting in a worst start-up behaviour and higher debris produced [8]. A major problem with this kind of application is to ensure an effective lubricant film and the oil must be synthetic if the oil sump is higher than 80 °C [9,10]. Oil analysis should be used to monitor the debris production and its causes as well as to ensure that the acidity, oxidation, viscosity and the water content are in accordance with the reference values.

Most wind turbine gearbox failures are rooted to the bearings [3–6]. The most significant fatigue wear phenomena are micropitting and smearing caused by large amounts of roller/raceway sliding in situations in which specific film thickness (Λ) is low, leading to high stresses and temperatures in the contact [11–14].

In the new global economy, it is mandatory to increase the efficiency of wind turbines, to reach the highest efficiency of gearbox drives and their parts and to minimize the power loss [15]. In order to increase gearbox efficiency it is important to quantify the main sources of power loss. The most common wind turbine gearboxes have planetary gears and the main losses occurring are: friction loss between the meshing teeth [16–21], friction loss in the bearings [16,22,23], friction loss in the seals [16,24], no-load gear losses [25–29] and energy loss due to air-drag [15].

Friction generated between the meshing teeth is the main source of power loss in a gearbox when the torque transmitted is high [30]. On a gearbox with low transmitted torque, the friction due to viscous forces of the lubricant on the seals, gears and bearings must be accessed in order to correctly predict the power loss. The energy loss due to no-load mechanisms is highly dependent on the lubricant viscosity. The meshing teeth power loss is influenced by the oil formulation and also by their ability to promote a lubricant film while keeping a low coefficient of friction.

Since the total torque loss is influenced by no-load and load losses, it is important to find a lubricant that promotes low friction

* Corresponding author. Tel.: +351 225082212.
E-mail address: cfernandes@inegi.up.pt (C.M.C.G. Fernandes).

0301-679X/$ - see front matter © 2013 Elsevier Ltd. All rights reserved.
http://dx.doi.org/10.1016/j.triboint.2013.10.003

in the contacts of the power transmitting components, which will lead to increased rolling bearings, gears and lubricant life. The physical properties of the lubricant should also lead to reasonably low no-load losses.

A back-to-back FZG test rig was used to investigate the torque loss influence of five ISO VG 320 fully formulated wind turbine gear oils.

The operating temperatures of the FZG test rig were monitored in eight different spots with thermocouples. Tests at 1.13, 2.26 and 6.79 m/s (pitch line speeds) were performed for different FZG standard load stages: K1, K5, K7 and K9 (arm lever = 0.35 m). Both gearboxes were jet-lubricated with an oil flow of 3 l/min. The oil jet input temperature was kept almost constant (80 ± 1 °C). Using the same geometry on both gearboxes, the torque loss generated by Type C40 gears was evaluated. Knowing the torque loss performance of the FZG drive gearbox standard gears allows the study of the torque loss performance for any configuration of the FZG test gearbox, including helical gears and/or angular contact bearings.

2. Wind turbine gear oils

In order to analyse the different gear oils suitable for the lubrication of wind turbine gearboxes, five fully formulated ISO VG 320 gear oils were selected.

In between the selected gear oils, five base oils can be found:

- Mineral base oil (MINR).
- Biodegradable ester base oil (ESTR).
- Polyalphaolephin base oil with an ester compatibiliser (PAOR).
- Hydroprocessed group III base oil with a PAMA thickener (MINE).
- Polyalkylene glycol (PAGD).

Table 1 displays the wind turbine gear oils physical properties as well as their chemical composition. A detailed description on the physical properties can be found in previous works with the same oils [31–34].

Table 1
Physical and chemical properties of wind turbine gear oils used.

Parameter Base oil	Unit [–]	MINR Mineral	ESTR Ester	PAOR Polyalphaolefin	MINE Mineral + PAMA	PAGD Polyalkyleneglycol
Chemical composition						
Zinc (Zn)	[ppm]	0.9	6.6	3.5	< 1	1
Magnesium (Mg)	[ppm]	0.9	1.3	0.5	< 1	1.4
Phosphorus (P)	[ppm]	354.3	226.2	415.9	460	1100
Calcium (Ca)	[ppm]	2.5	14.4	0.5	2	0.8
Boron (B)	[ppm]	22.3	1.7	28.4	36	1.0
Sulphur (S)	[ppm]	11200	406	5020	6750	362
Physical properties						
Density@15 °C	[g/cm^3]	0.902	0.915	0.859	0.893	1.059
Thermal expansion coefficient ($\alpha_t \times 10^{-4}$)	[/]	−5.8	−8.1	−5.5	−6.7	−7.1
Viscosity @ 40 °C	[cSt]	319.22	302.86	313.52	328.30	290.26
Viscosity @ 70 °C	[cSt]	65.81	77.48	84.99	93.19	102.33
Viscosity @ 100 °C	[cSt]	22.33	34.85	33.33	37.13	51.06
m	[/]	9.066	7.582	7.351	7.048	5.759
n	[/]	3.473	2.880	2.787	2.663	2.151
Thermoviscosity @ 40 °C ($\beta \times 10^{-3}$)	[K^{-1}]	63.88	49.09	50.68	49.33	37.34
Thermoviscosity @ 70 °C ($\beta \times 10^{-3}$)	[K^{-1}]	42.83	35.25	36.16	35.48	28.36
Thermoviscosity @ 100 °C ($\beta \times 10^{-3}$)	[K^{-1}]	30.07	26.19	26.72	26.40	22.12
s @ 0.2 GPa	[/]	0.9904	0.6605	0.7382	0.7382	0.5489
t @ 0.2 GPa	[/]	0.1390	0.1360	0.1335	0.1335	0.1485
Piezoviscosity @ 40 °C ($\alpha \times 10^{-8}$)	[Pa^{-1}]	2.207	1.437	1.590	1.600	1.278
Piezoviscosity @ 70 °C ($\alpha \times 10^{-8}$)	[Pa^{-1}]	1.774	1.212	1.339	1.353	1.105
Piezoviscosity @ 100 °C ($\alpha \times 10^{-8}$)	[Pa^{-1}]	1.527	1.071	1.182	1.197	0.988
VI	[/]	85	140	150	163	230

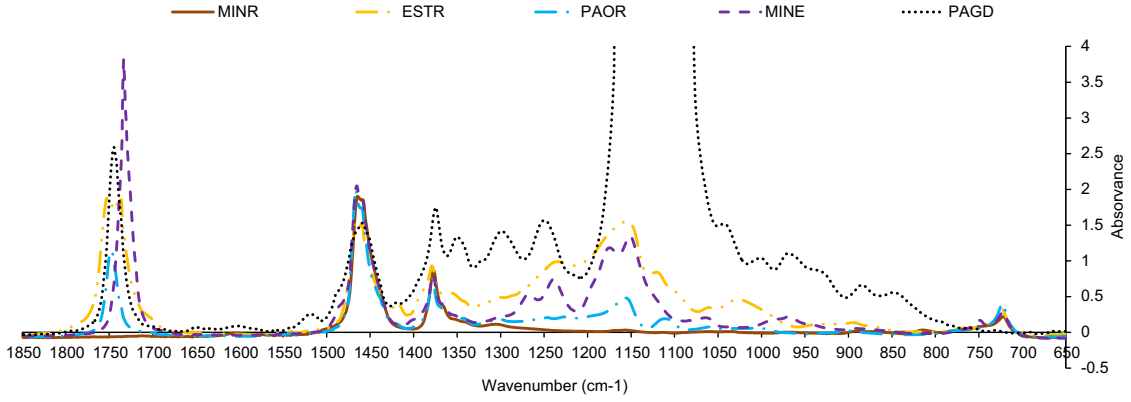

Fig. 1. IR spectrum.

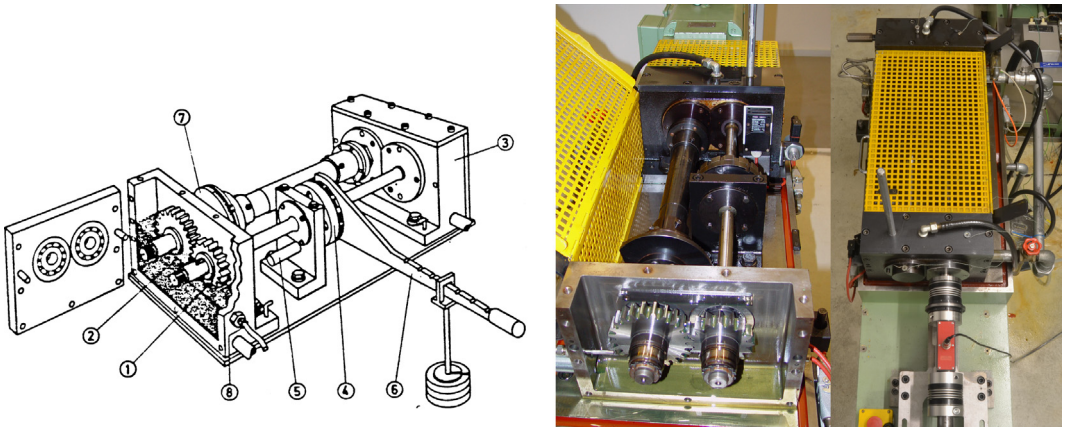

Fig. 2. Schematic view of the FZG gear test rig.

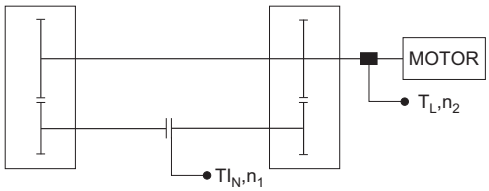

Fig. 3. Schematic view of the FZG gear test rig.

Table 2
Technical specifications of the ETH DRDL torque cell.

Torque transducer type DRDL	
Nominal torque (N m)	50
Measurement range (N m)	5/10/20/50
Non-linearity (%)	<0.1
Hysteresis (%)	<0.1
Accuracy (%)	0.01
Temperature sensitivity (%/K)	0.01
Torque measuring module type ValueMaster$_{Base}$	
Accuracy (%)	0.02
Non-linearity (%)	0.1
AD converter resolution	11 bit+1 bit for leading sign

The FTIR analysis was used in order to identify some of the characteristic peaks of the lubricants (see Fig. 1).

3. Test rig

Fig. 2 presents the FZG test machine used in this work. The FZG machine is a gear test rig with circulating power due to a static torque applied [35]. Test pinion (1) and wheel (2) are connected by two shafts to the drive gearbox (3). The shaft connected to test pinion (1) is divided into two parts by the load clutch (4). One-half of the clutch can be fixed with the locking pin (5), whereas the other can be twisted using the load lever and different weights (6).

The torque loss (T_L) was measured using a ETH Messtechnik DRDL II torque transducer assembled on the FZG test machine, as shown schematically in Fig. 3. The technical characteristics of the sensor are displayed in Table 2. The system uses a sensor interface (*Valuemaster$_{Base}$*) to communicate with a PC or Notebook with a Ethernet connection. The integration of the torque cell with the software allows to record the torque values with an adjustable sampling rate (from 1 to 1000 Hz).

The operating temperatures on eight different points of the assembly were also measured using Type K thermocouples. The temperatures were recorded during each test using a software and a sampling rate of 1 Hz.

Table 3
Geometry of the C40 test gears.

Gear type	**Type C40**	
	Pinion	**Wheel**
Number of teeth	16	24
Module (mm)	4.5	
Centre distance (mm)	91.5	
Pressure angle (°)	20	
Face width (mm)	**40**	
Addendum modification (/)	+0.1817	+0.1715
Addendum diameter (mm)	82.64	118.54
Transverse contact ratio ε_α (/)	1.44	
Material	20MnCr5	

Table 4
Roughness parameters of the C40 spur gear before and after run-in.

			Ra	Rq	Rz	Rmax	Rpk	Rk	Rvk
New	Pinion	Axial	0.3	0.3	1.5	1.9	0.3	1	0.4
		Radial	1.1	1.4	7.8	9.4	1.3	3.1	2
	Wheel	Axial	0.2	0.3	1.1	1.9	0.3	0.6	0.3
		Radial	0.8	1.1	4.9	6	0.9	2.5	1.2
Run-in	Pinion	Axial	0.4	0.5	2.5	3.3	0.4	1	0.8
		Radial	1	1.3	5.8	8.4	0.6	2.3	2.7
	Wheel	Axial	0.3	0.3	1.8	2.3	0.3	0.9	0.5
		Radial	0.7	0.9	4.5	5.7	0.6	2	1.5

4. Drive and test gearboxes

4.1. Gears

The torque loss tests performed in this work used type C gears with a face width of 40 mm usually assembled on FZG drive gearboxes. Table 3 displays the main geometric properties of the C40 gears.

The same C40 gear set was used for testing all the lubricants. To ensure that a similar surface finish was used with all lubricants, the C40 gear was run-in during 48 h under dip lubrication with a PAO 150 gear oil (Table 4).

The surface roughness was evaluated before and after the run-in period. Figs. 4 and 5 display tooth flank profiles measured before and after the run-in, in the axial and radial direction, respectively. The surface roughness in the radial direction is considerably larger than that in the axial direction due to the grinding direction (axial).

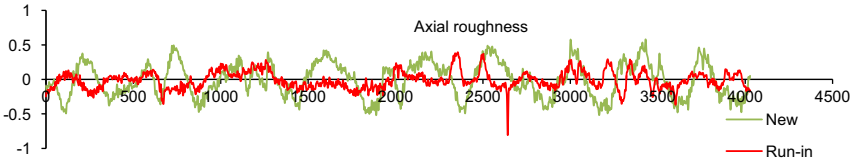

Fig. 4. Axial roughness of the pinion before and after the run-in.

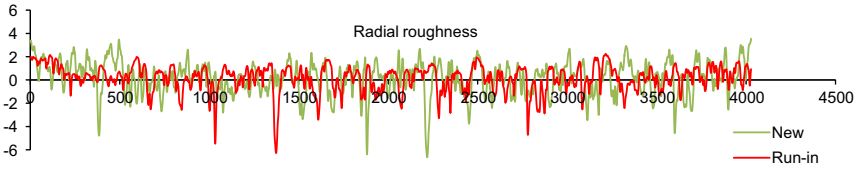

Fig. 5. Radial roughness of the pinion before and after the run-in.

Table 5
Operating conditions on the torque loss tests performed. Load stages with a load lever arm of 0.35 m.

Load stage	Wheel torque (N m)	Wheel speed (rpm)	v_t (m/s)	Power (W)	F_{bt} (N)	F_r (N)	p_H (MPa)
K1	4.95	200	1.131	103.7	98	37.2	108.14
		400	2.262	207.3			
		1200	6.786	622.0			
K5	104.97	200	1.131	2198.5	2069	789.6	497.98
		400	2.262	4396.9			
		1200	6.786	13190.9			
K7	198.68	200	1.131	4161.2	3915	1494.5	685.11
		400	2.262	8322.4			
		1200	6.786	24 967.2			
K9	323.27	200	1.131	6770.4	6371	2431.6	873.90
		400	2.262	13 540.9			
		1200	6.786	40 622.7			

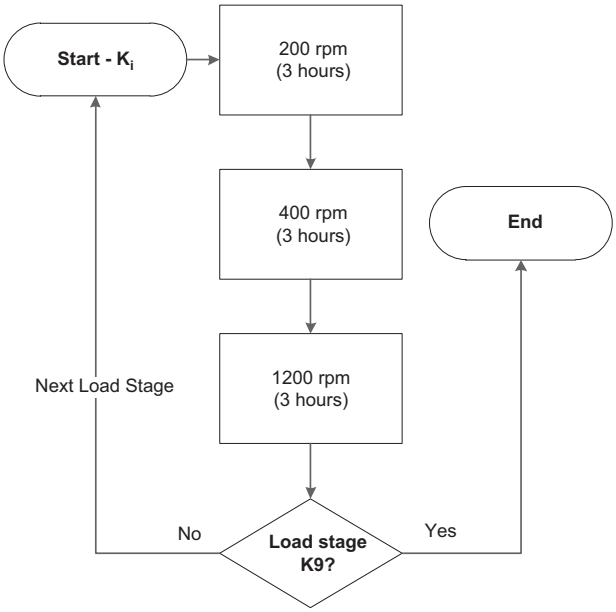

Fig. 6. Test procedure sequence.

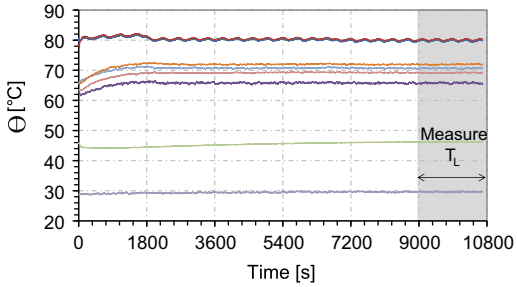

Fig. 7. Temperatures behaviour on the test machine with steady state conditions.

4.2. Rolling bearings and seals

The shafts on the test and slave gearbox are supported with cylindrical roller bearings (NJ 406). The rolling bearings have a dynamic load capacity of $C=60.5$ kN and a static load capacity of $C_0=53$ kN.

The gearboxes are sealed with four Viton lip seals with an internal diameter of $d_{sh}=30$ mm. A Viton lip seal is also assembled on the drive gearbox motor shaft ($d_{sh}=26$ mm).

5. Test procedure

The operating conditions used in the torque loss tests are displayed in Table 5. The tangential speed, the power circulating in the system, the tangential force transmitted by the gears, the radial forces on the rolling bearings and the Hertz pressure in the gears are also included. The oil volumetric flow was set to 3 l/min at a temperature of 80 °C.

The test procedure can be summarized as follows:

1. Run load stage Ki and rotational speed condition (Table 5) during 3 h according to the test sequence presented in Fig. 6:
   - Register the assembly working temperatures.

- Continuous torque measurement with a sample rate of 1 measurement per s.

2. Repeat procedure till the highest load stage.

The values presented for torque loss and temperature are the average of the last 30 min of operation, i.e. only the steady state operating conditions are considered for the average calculation (see Fig. 7). Between each oil tested the gearboxes were flushed with solvent. The oil reservoir and the injection system are completely drained and cleaned with a solvent (the solvent used depends on the oil base).

6. Experimental results

6.1. Torque loss

This section presents the results for the total torque loss measurements for all the test conditions. Table 6 displays the torque loss (T_L) measurements for all the lubricants and test conditions.

Fig. 8 displays the torque loss measured for load stage K1 at the input speeds of 200, 400 and 1200 rpm. These test conditions were performed to gather knowledge about the torque loss for a no-load condition, i.e. the results presented are mainly promoted by load independent losses.

MINE oil generated the lower friction torque loss when load stage K5 was applied, no matter the rotational speed selected. At 200 and 400 rpm the MINR generated much higher torque loss than the other formulations. At 1200 rpm the no-load losses of the PAGD oil are higher resulting in highest total torque loss generated (see Fig. 8).

For the tests performed at load stage K7 the higher torque loss is achieved for the MINR oil. At low speed (200 and 400 rpm) the higher viscosity index of the PAGD keeps the torque loss lower than other oil formulations. At 1200 rpm all lubricants increase the torque loss.

Table 6
Total torque loss [N m] for each test condition.

Speed	K_{FZG}	MINR	MINE	ESTR	PAOR	PAGD
200	K1	1.16	1.24	1.24	1.22	1.38
	K5	3.72	2.97	3.14	3.12	3.08
	K7	5.92	5.32	4.85	5.08	4.70
	K9	8.88	8.08	7.56	7.73	7.00
400	K1	1.50	1.56	1.53	1.37	1.73
	K5	3.77	3.14	3.30	3.23	3.33
	K7	5.75	5.27	4.85	4.95	4.79
	K9	8.54	7.93	7.33	7.21	6.65
1200	K1	2.13	2.22	2.21	2.13	2.25
	K5	4.22	3.88	4.11	4.06	4.42
	K7	5.86	5.35	5.36	5.55	5.76
	K9	8.08	7.84	7.31	7.34	7.19

Table 7
Temperature of oil leaving the test gearbox.

		MINR	ESTR	PAOR	MINE	PAGD
200	K1	77.2	78.2	79.6	77.6	79.2
	K5	77.3	77.5	79.2	77.8	78.3
	K7	77.7	78.1	79.5	77.7	78.5
	K9	77.7	78.2	78.9	78.1	78.4
400	K1	78.6	77.8	79.2	78.0	79.0
	K5	78.9	78.1	79.0	78.0	79.2
	K7	78.5	78.4	78.8	78.5	78.9
	K9	78.4	78.8	78.9	78.7	79.0
1200	K1	80.4	79.6	79.9	79.5	79.7
	K5	80.5	79.9	80.1	79.7	79.6
	K7	81.8	81.0	80.5	81.2	80.1
	K9	83.9	82.2	80.7	82.1	80.9

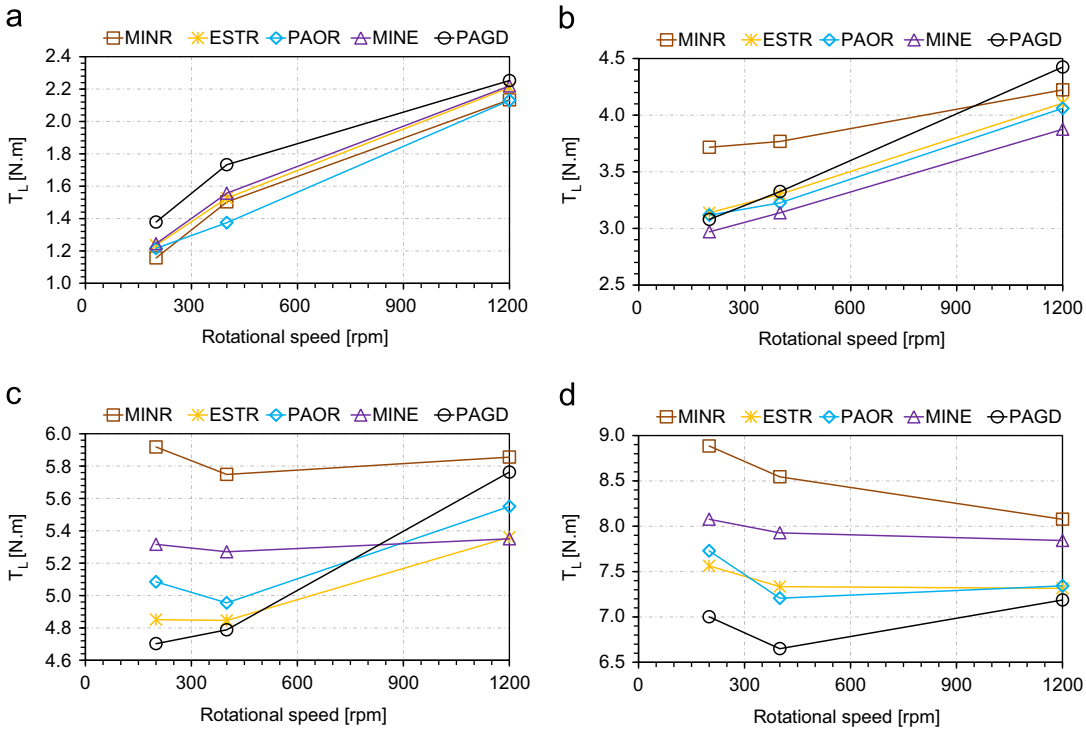

Fig. 8. Total torque loss results. (a) K1 load stage; (b) K5 load stage; (c) K7 load stage; (d) K9 load stage.

Table 8
Efficiency values [%] calculated for test gearbox.

Speed	K_{FZG}	MINR	MINE	ESTR	PAOR	PAGD
200	K1	87.54	86.52	86.63	86.85	84.94
	K5	98.21	98.58	98.49	98.50	98.52
	K7	98.50	98.65	98.77	98.71	98.81
	K9	98.62	98.74	98.82	98.80	98.91
400	K1	83.45	82.80	83.16	84.99	80.62
	K5	98.19	98.49	98.41	98.45	98.40
	K7	98.54	98.66	98.77	98.75	98.79
	K9	98.67	98.77	98.86	98.88	98.97
1200	K1	75.43	74.27	74.41	75.48	73.82
	K5	97.97	98.14	98.02	98.05	97.87
	K7	98.52	98.64	98.64	98.59	98.54
	K9	98.74	98.78	98.86	98.86	98.88

For load stage K9 the PAGD oil generate much lower torque loss than the other formulations. As speed increases the differences between the oils become smaller. The MINR is benefited due to the lubrication regime transition and the PAGD is penalized due to their higher viscosity generating higher no-load losses.

6.2. Test rig temperatures

The temperature of the oil leaving the test gearbox is displayed in Table 7 for all oils and test conditions. These results show that the increase in speed promotes an higher increase of temperature than an increase of load.

It is also interesting to observe the stabilization temperature of the test rig base plate (ϑ_{stab_base}) that is calculated according to Eq. (1). It was verified that for the same operating conditions, the difference between the maximum and the minimum stabilization temperature is quite smaller, usually smaller than 1 °C, whatever the lubricating oil considered

$$\vartheta_{stab} = \vartheta_{base} - \vartheta_{room} \tag{1}$$

7. Gearboxes efficiency

The calculation of the gearbox efficiency in a closed loop test rig is a function of the static torque installed in the system and the torque applied by the driving motor (designated as torque loss in this work T_L). A static torque was applied on the pinion shaft T_{IN} (see Fig. 3), as a result, the wheel shaft has an higher torque T_W, related with the pinion torque by the transmission ratio ($i = Z_2/Z_1$), as represented by Eq. (2). The wheel shaft torque values tested are already presented in Table 5

$$T_W = i \cdot T_{IN} \tag{2}$$

The torque loss (T_L), or the torque applied by the electric motor, was measured on the wheel shaft. Thus, the efficiency of the test rig is given by

$$\eta_{global} = \eta_D \times \eta_T = \frac{T_W - T_L}{T_W} \times 100 \tag{3}$$

The test and slave gearboxes have the same gears and so it is assumed that both gearboxes have the same efficiency.

So, the efficiency of the drive gearbox (η_D) is equal to the efficiency of the test gearbox (η_T) that are calculated according to the below equation

$$\eta_D = \eta_T = \sqrt{\frac{T_W - T_L}{T_W}} \times 100 \tag{4}$$

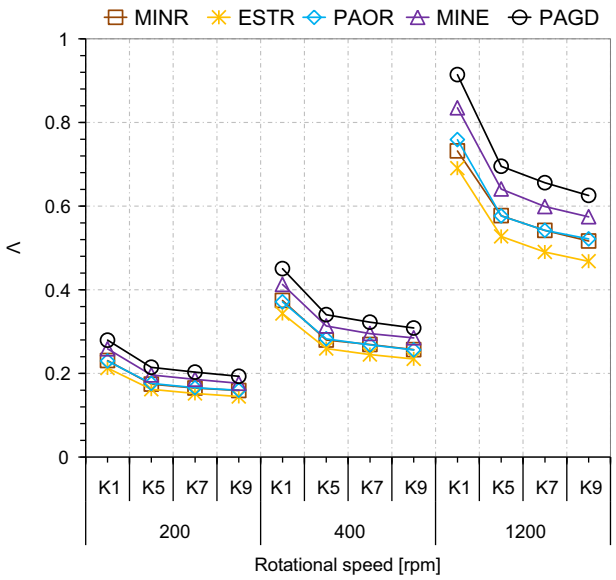

Fig. 9. Specific film thickness between gear tooth.

Table 8 displays the efficiency values calculated for a single gearbox (see Eq. (4)) for all the lubricants tested.

8. Specific film thickness between gear tooth

The flash and bulk temperatures were calculated according to DIN 3990. The bulk temperature will allow the determination of oil temperature in the inlet zone and thus to determine the lubricant properties (β, α and η) and the film thickness (h_{0C}) at bulk temperature

$$\vartheta_{flash} = 0.08 T_1^{1.2} \left(\frac{100}{\nu_{40}}\right)^{\nu_{40}^{-0.4}} \tag{5}$$

$$\vartheta_{bulk} = XS \cdot (\vartheta_{oil} + C1 \cdot \vartheta_{flash_{int}}) \tag{6}$$

With $XS = 1.2$, for jet-lubrication; $XS = 1$, for dip lubrication and $C1 = 0.7$. T_1 represents the torque applied on the pinion shaft.

The centre film thickness in the gears contact was determined using the Dowson and Higginson [36] equation for linear contacts

$$h_0 = 0.975 \cdot R_X \cdot U^{0.727} \cdot G^{0.727} \cdot W^{-0.091} \tag{7}$$

The parameters U, G and W calculated according to Eqs. (8), (9) and (10), respectively

$$U = \frac{\eta_{bulk} \cdot (U_1 + U_2)}{2 \cdot R_X \cdot E^*} \tag{8}$$

$$G = 2 \cdot \alpha_{bulk} \cdot E^* \tag{9}$$

$$W = \frac{F_n}{R_X \cdot l \cdot E^*} \tag{10}$$

The theoretical film thickness was calculated at the operating pitch radius, as well as, the oil properties at the corresponding operating bulk temperatures.

The theoretical film thickness h_0 was corrected using the thermal reduction factor (ϕ_T) due to inlet shear heating, as shown in Eqs. (11)– (15). The specific film thickness was calculated with Eq. (15), taking into account the composite roughness of the contact ($\sigma \approx 1$ μm, as shown in Section 4)

$$h_{0C} = \phi_T \cdot h_0 \tag{11}$$

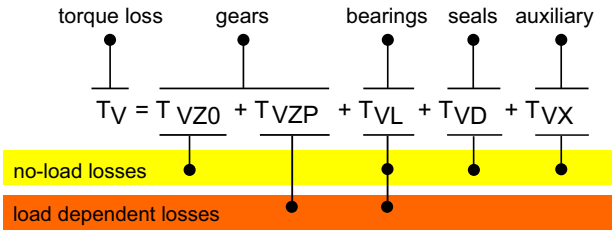

Fig. 10. Torque loss contributions [37].

$$\phi_T = \{1+0.1\cdot(1+14.8S^{0.83})\cdot L^{0.64}\}^{-1} \tag{12}$$

$$L = \frac{\beta\cdot\eta_{bulk}\cdot(U_1+U_2)^2)}{K} \tag{13}$$

$$S = \frac{|U_1-U_2|}{U_1+U_2} \tag{14}$$

$$\Lambda = \frac{h_{0C}}{\sqrt{\sigma_1^2+\sigma_2^2}} \tag{15}$$

The specific film thickness for each test condition is displayed in Fig. 9. The specific film thickness is quite similar for all oils because they have a similar lubricant parameter ($LP=\alpha_{bulk}\cdot\eta_{bulk}$) at corresponding bulk temperatures. The small differences between oils are due to the differences in the operating viscosity, but those differences are not enough to promote a different lubrication regime.

The specific film thickness allows to access the lubrication regime of the contacting teeth at the pitch point. All the tests are performed on boundary lubrication, except the test performed at K1-1200 rpm that is performed under mixed film lubrication ($\Lambda>0.7$).

9. Torque loss model

The torque losses occurring within a gearbox are due to different mechanical sources. On this work the losses that were considered are represented in Fig. 10. Note that the gears losses are divided in load dependent losses (T_{VZP}) and load independent losses (T_{VZ0}).

9.1. No-load losses

9.1.1. Gear no-load losses

The no-load torque loss generated by gears in the case of jet-lubrication is a sum of different loss mechanisms (see Eq. (16)), where $T_{VZ,Q}$ is the loss due to oil squeeze, caused by the displacement of the oil in the contact area between gear tooth [26]. The loss of air drag $T_{VZ,V}$ is due to air or oil mist and is known as ventilation loss [27]. The oil steam in jet-lubrication causes the impulse loss torque $T_{VZ,I}$ [25]

$$T_{VZ0} = T_{VZ0,Q}+T_{VZ0,I}+T_{VZ0,V} \tag{16}$$

The no-load losses were determined for each input speed using the torque loss measured on load stage K1. The no-load losses remain similar for higher load stages.

The no load-losses are calculated subtracting the gear mesh losses, the rolling bearing losses and the seal losses to the total torque loss on load stage K1 as represented in the below equation

$$T_{VZ0} = T_L^{K1}-T_{VZP}^{K1}-T_{VL}^{K1}-T_{VD}^{K1} \tag{17}$$

Note that T_{VZP}^{K1} is very close to zero, so this term was disregarded.

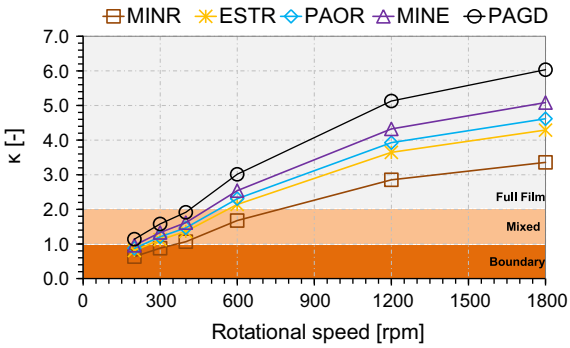

Fig. 11. Viscosity ratio of the rolling bearing.

Table 9
Sliding coefficient of friction (μ_{sl}).

Oil	$\kappa<1$	$1<\kappa<2$	$\kappa>2$
MINR	0.0339	0.0243	0.0192
ESTR	0.0332	0.0225	0.0099
PAOR	0.0347	0.0203	0.0112
MINE	0.0332	0.0259	0.0099
PAGD	0.0208	0.0141	0.0112

9.1.2. Seal losses – T_{VD}

The torque loss of the shaft seals is due to the friction between the sealing lip and the rotating shaft. The equation proposed by Freudenberg was used as shown below

$$T_{VD} = 7.69\cdot10^{-6}d_{sh}\cdot\frac{30}{\pi} \tag{18}$$

9.2. Load dependent losses

9.2.1. Rolling bearings – T_{VL}

In order to understand the torque loss behaviour of the rolling bearings the model proposed by SKF [23] was used. The friction torque model used allow to quantify the different components of the friction torque.

The total friction torque is the sum of four different physical sources of torque loss, represented by the below equation

$$T_{VL} = M_{rr}^{'}+M_{sl}+M_{drag}+M_{seals} \tag{19}$$

The four sources of torque loss considered by the model are

- Rolling torque ($M_{rr}^{'}$).
- Sliding torque (M_{sl}).
- Drag torque (M_{drag}).
- Seals (M_{seals}).

The rolling bearings assembled in the test rig (NJ 406 MA) don't have seals, so the seal losses were not considered. See Appendix A for further explanation on the equations used for the rolling bearing studied.

The lubrication regime of the rolling bearings was calculated using the SKF viscosity ratio [23] given by the below equation

$$\kappa = \frac{\nu}{\nu_1} \tag{20}$$

The viscosity ratio is plotted in Fig. 11. The rotational speeds presented correspond to pinion and wheel shaft. The lubrication regime is divided into

- Boundary lubrication ($\kappa<1$).
- Mixed lubrication ($1<\kappa<2$).
- Full film lubrication ($\kappa>2$).

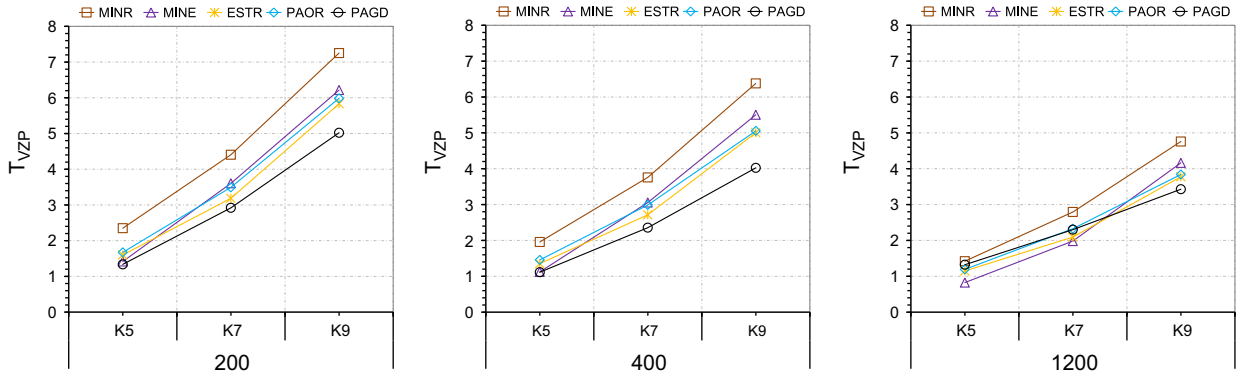

Fig. 12. Torque loss due to gear meshing.

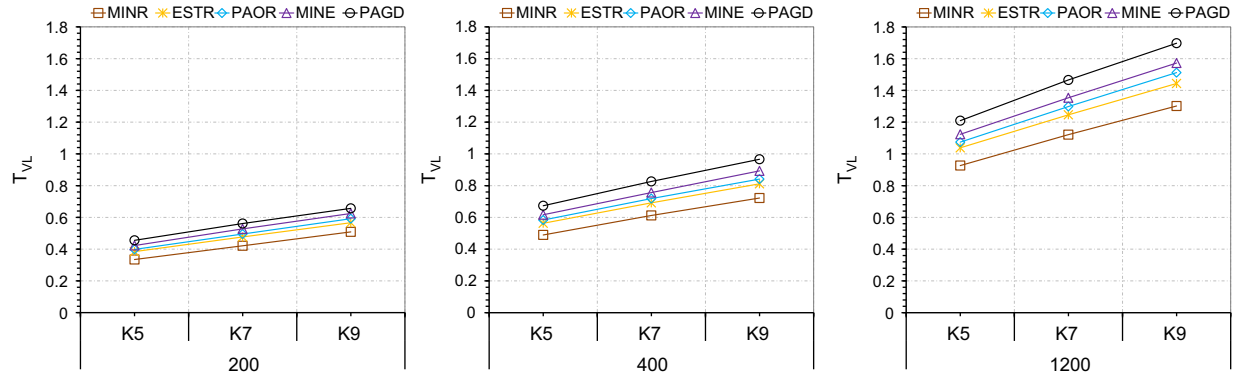

Fig. 13. Torque loss due to rolling bearings.

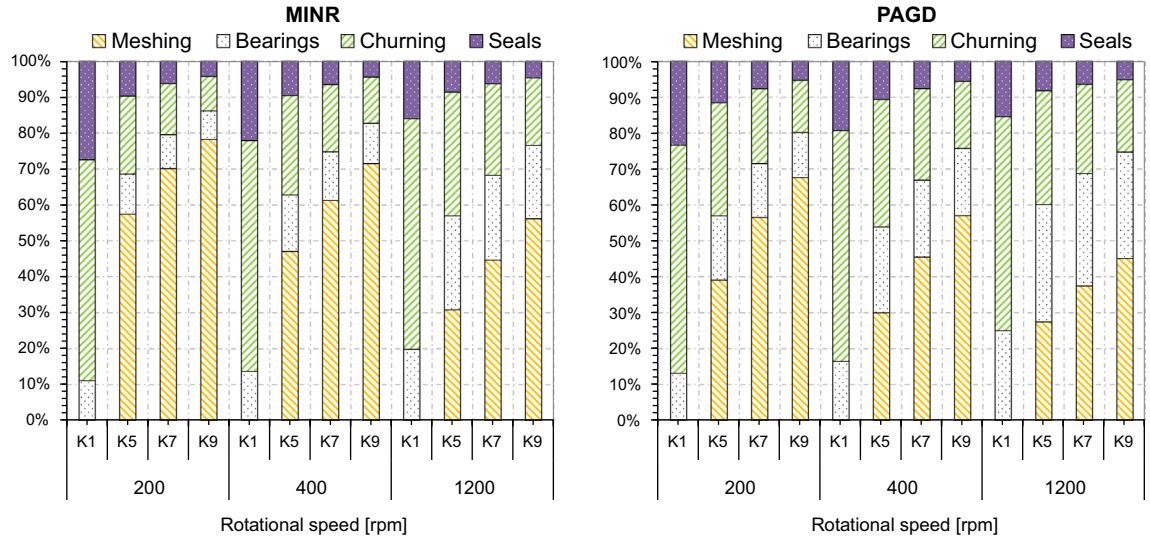

Fig. 14. Torque loss sources influence on total torque loss of MINR and PAGD oils.

The sliding coefficient of friction (μ_{sl}) used for each lubricant was determined experimentally with the results published in [31]. To apply the results determined previously for this rolling bearing the viscosity ratio was used, defining 3 different lubrication regimes within the experimental results. In this way each sliding coefficient of friction used is presented in Table 9 for each oil.

Further explanation on the subject is presented in previous works [31–34].

9.3. *Meshing gears – T_{VZP}*

Ohlendorf [38] first introduced an approach for the load dependent losses of spur gears. The torque loss generated between gear tooth contact can be calculated using the below equation

$$T_{VZP} = T_{IN} H_V \mu_{mZ} \tag{21}$$

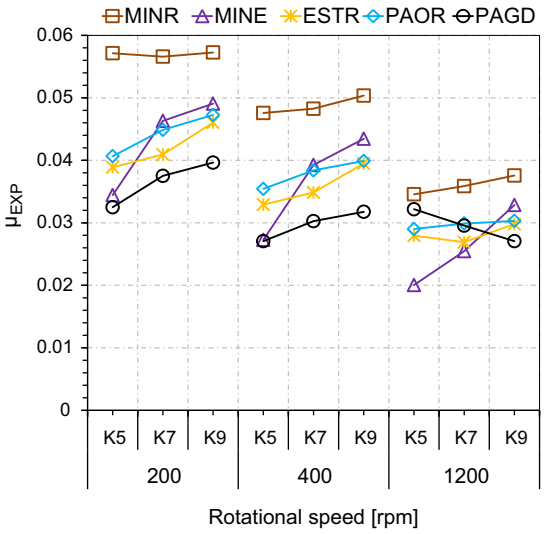

Fig. 15. Coefficient of friction.

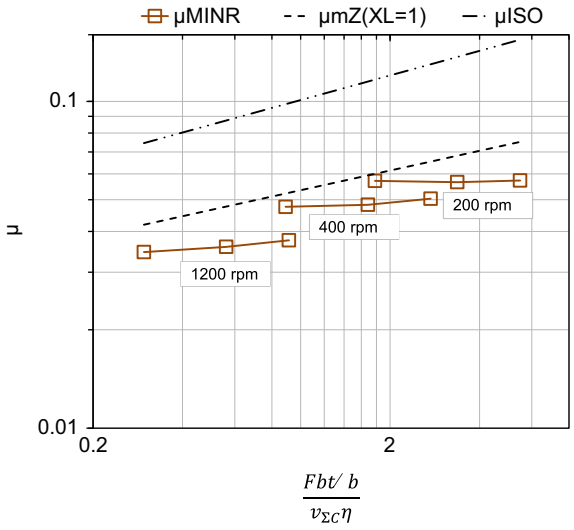

Fig. 16. Coefficient of friction comparison.

where H_V represents the gear loss factor which is determined according to the below equation

$$H_V = \frac{\pi(u+1)}{z_1 u \cos\beta_b}(1-\varepsilon_\alpha+\varepsilon_1^2+\varepsilon_2^2) \tag{22}$$

This formula assumes that the coefficient of friction (μ_{mZ}) is constant along the path of contact and that the tangential force (F_{bt}) is almost constant for the geometry used. In fact this is a simplification of the problem.

The gear load losses for any load stage and input speed are calculated according to Eq. (23), subtracting the rolling bearing losses, the seal losses and the no-load losses previously calculated to the total experimental torque loss (Eq. (17))

$$T_{VZP}^{Ki} = T_L^{Ki} - T_{VL}^{Ki} - T_{VD}^{Ki} - T_{VZ0}^{K1} \tag{23}$$

9.4. Torque loss model results

The torque loss sources were quantified for each oil and an analysis is presented in this section.

In Fig. 12 the torque loss generated by the meshing gears is presented for each test condition and for each oil. The MINR oil always generated higher torque loss no matter what rotational speed is used. The PAGD oil generated lower torque loss for 200 and 400 rpm for all load stages. For 1200 rpm the MINE oil for K5 and K7 generated the lowest torque loss. As expected the increase in the rotational speed reduced the torque loss generated on the gears for all the lubricants due to film thickness formation, as can be seen in Fig. 9, where some oils at 1200 rpm have a lubrication regime transition from boundary lubrication to mixed lubrication. Both PAOR and ESTR performed very similar for all the sources of the torque loss, and are scored in between the MINR and PAGD oils. It should be noted that at low loads MINE can generate lower gear mesh losses than PAGD. When the applied torque increases MINE also shows the higher gear mesh load losses than any of the other tested synthetic gear oils.

The torque loss generated by the rolling bearings is higher when the speed is increased, for all oils. The oils with higher viscosity index generated higher losses on the rolling bearings. This behaviour is expected because at mixed and full film conditions the rolling torque is the most influential component on rolling bearings torque loss (see Figs. 11 and 13).

The influence of each torque loss source is presented in Fig. 14 for MINR and PAGD oils. The influence of the no-load losses is higher on the PAGD oil as expected. The influence of load dependent gear losses is the main explanation for the differences verified between the MINR and PAGD oils.

Table 10
XL lubricant parameter.

Oil	XL
MINR	0.89
PAOR	0.65
ESTR	0.63
MINE	$0.5\left(\frac{F_{bt}/b}{\nu_{\Sigma C}\rho_{redC}}\right)^{0.1}$
PAGD	$0.5\left(\frac{F_{bt}/b}{\nu_{\Sigma C}\rho_{redC}}\right)^{0.05}$

10. Coefficient of friction on meshing gears

Schlenk [39] proposed Eq. (24) for the average coefficient of friction along the path of contact. The lubricant parameter XL is equal to 1 for non-additivated mineral oils

$$\mu_{mZ} = 0.048\left(\frac{F_{bt}/b}{\nu_{\Sigma C}\rho_{redC}}\right)^{0.2}\eta^{-0.05}Ra^{0.25}X_L \tag{24}$$

The ISO standard defines Eq. (25) for the average coefficient of friction between meshing tooth

$$\mu_{ISO} = 0.143\left(\frac{F_{bt}/b\cdot Ra}{\nu_{\Sigma C}\rho_{redC}\eta}\right)^{0.25} \tag{25}$$

The experimental coefficient of friction was calculated using the below equation

$$\mu_{EXP} = \frac{T_{VZP}}{T_{IN}H_V} \tag{26}$$

In Fig. 15 the coefficient of friction on the meshing gears for each oil tested is presented. The MINR always generated the highest coefficient of friction.

A comparison between the coefficient of friction determined experimentally and the values given by Eqs. (24) and (25) was done in Fig. 16 as a function of the hydraulic parameter $(F_{bt}/b)/\nu_{\Sigma C}\eta$. The results suggested that the Schlenk equation gives a good correlation with the coefficient of friction derived from the experimental results.

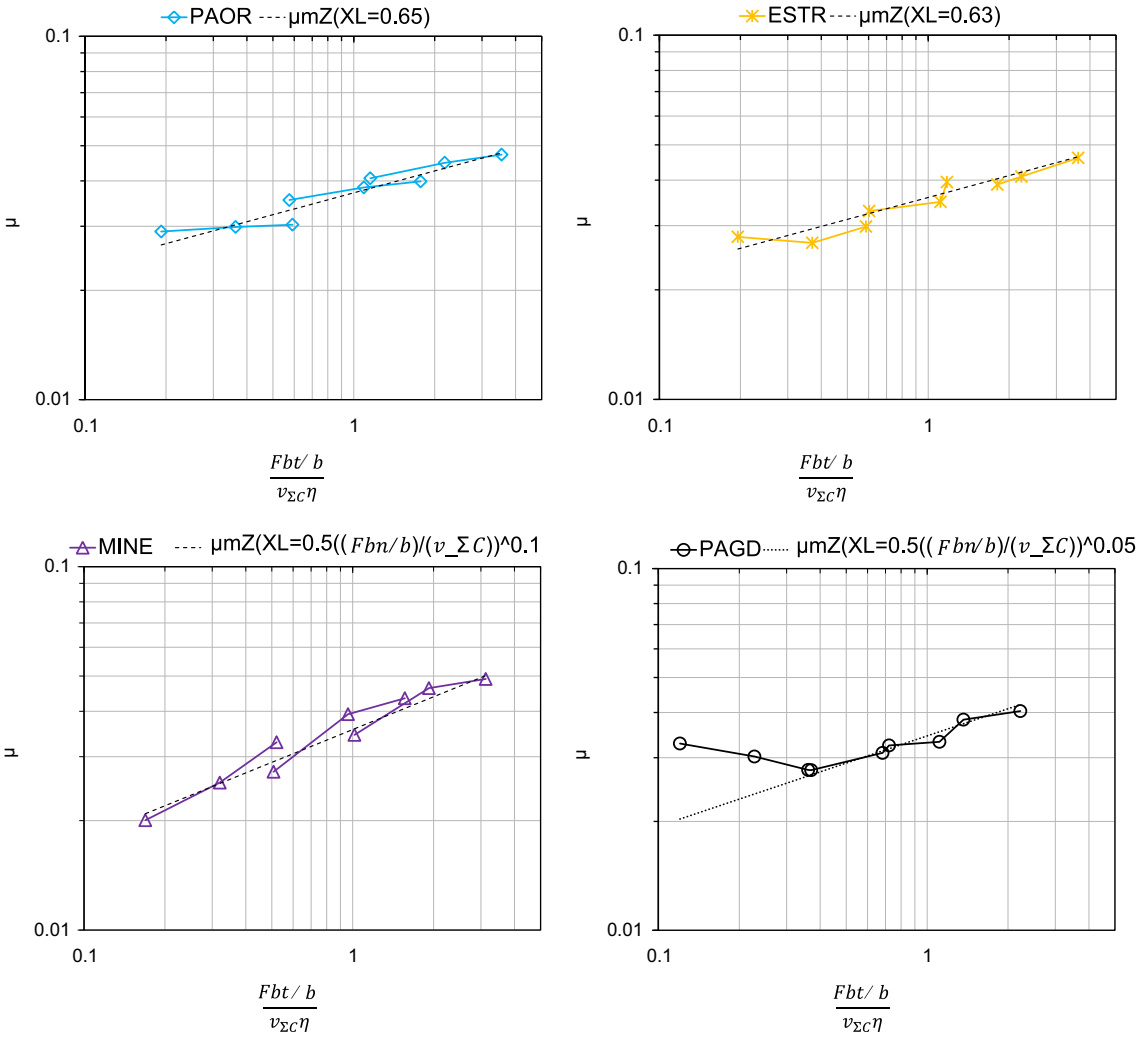

Fig. 17. Comparison between coefficient of friction determined experimentally and the Schlenk equation with XL parameter.

In order to use the Schlenk equation to predict the torque loss generated by the tested wind turbine gear oils, the lubricant parameter was determined for each case. For MINR, PAOR and ESTR the XL parameter can be given by a constant value. The PAGD and MINE oils have an evolution with load and speed different from the one suggested by the Schlenk equation, so the XL parameters presented in Table 10 are suggested. The XL coefficient for MINR is close to, but lower than 1. This result was expected since XL=1 for non-additivated mineral oils (MINR is fully formulated).

In Fig. 17 is presented the experimental coefficient of friction and the coefficient of friction of the Schlenck equation corrected with the XL parameter of Table 10 for PAOR, ESTR, MINE and PAGD oils.

11. Conclusions

The results achieved with this work showed that:

- The PAGD oil can reduce more than 20% the torque loss generated with MINR.
- There is a reduction of 10% in the torque loss generated by PAGD, when compared to the other synthetic gear oils.
- PAGD shows a 30% reduction on the torque loss between the meshing teeth in comparison to MINR (at high loads).
- MINR showed the lowest no load loss.
- At low load MINE shows the lowest gear mesh torque loss.
- The benefits (torque loss) of using the best relative to the worst performing lubricant diminish with increasing speeds (21–11%).
- For high loads, the performance of the ESTR and PAOR oils was very similar.
- The coefficient of friction determined experimentally follows the behaviour proposed by the literature.
- The methods used for the tests performed are valid to score the torque loss performance of the different wind turbine gear oils.

Acknowledgements

The authors acknowledge to “Fundação para a Ciência e Tecnologia” for the financial support given through the project “High efficiency lubricants and gears for windmill planetary gearboxes”, with research contract PTDC/EME-PME/100808/2008.

Appendix A. Rolling bearing friction torque model

Eqs. (A.1)–(A.9) define the rolling, sliding and drag torques. The seal loss of rolling bearings was not considered because the

Table A1
SKF rolling bearing constants.

	Cylindrical roller bearing (NJ 406 MA)
R_1	1.00×10^{-6}
S_1	0.16
S_2	0.0015
K_Z	5.1
K_L	0.65

NJ 406 MA rolling bearing does not have seals

$$M_{rr} = \phi_{ish} \cdot \phi_{rs}[G_{rr}(n \cdot \upsilon)^{0.6}] \tag{A.1}$$

$$\phi_{ish} = \frac{1}{1+1.84 \times 10^{-9}(nd_m)^{1.28}\nu^{0.64}} \tag{A.2}$$

$$\phi_{rs} = \frac{1}{e^{K_{rs}\nu n(d+D)\sqrt{\frac{K_z}{2(D-d)}}}} \tag{A.3}$$

$$G_{rr} = R_1 \cdot d_m^{2.41} \cdot F_r^{0.31} \tag{A.4}$$

$$M_{sl} = G_{sl} \cdot \mu_{sl} \tag{A.5}$$

$$G_{sl} = S_1 \cdot d_m^{0.9} \cdot F_a + S_2 \cdot d_m \cdot F_r \tag{A.6}$$

$$\mu_{sl} = \phi_{bl} \cdot \mu_{bl} + (1-\phi_{bl}) \cdot \mu_{EHD} \tag{A.7}$$

$$\phi_{bl} = \frac{1}{e^{2.6 \times 10^{-8}(n\cdot\nu)^{1.4}d_m}} \tag{A.8}$$

$$M_{drag} = 10 \cdot V_M \cdot K_{roll} \cdot B \cdot d_m^4 \cdot n^2 \tag{A.9}$$

$$K_{roll} = \frac{K_L \cdot K_Z \cdot (d+D)}{D-d} \times 10^{-12} \tag{A.10}$$

$$V_M = 14.9 \times 10^{-5} \tag{A.11}$$

The constants used on the calculation are given in Table A1.

References

[1] High efficiency planetary gearboxes for eco-power. World Pumps 2001;2001 (419):34:34–36, http://dx.doi.org/10.1016/S0262-1762(01)80327-8.
[2] E.E. Agency. Europe's onshore and offshore wind energy potential—an assessment of environmental and economic constraints. EEA Technical Report. No. 6; 2009. p. 91.
[3] McNiff B, Musial W, Errichello R. Variations in gear fatigue life for different wind turbine braking strategies. Prepared for AWEA wind power '90. Washington, DC; 24–28 September 1990 (1991). 10p. [Medium: ED; Size].
[4] Winkelmann L. Surface roughness and micropitting. In: National renewable energy laboratory wind turbine tribology seminar; 2011.
[5] McDade M. Gearbox reliability collaborative (GRC) failure database, In: National renewable energy laboratory wind turbine tribology seminar; 2011.
[6] Jungk M. Update on the development of a full life wind turbine gear box lubricating fluid. In: National renewable energy laboratory wind turbine tribology seminar; 2011.
[7] Tavner PJ, Spinato F, Bussel GJWv, Koutoulakos E. Reliability of different wind turbine concepts with relevance to offshore application. Presented at the European wind energy conference.
[8] Zellmann J. Main types of damage to wind turbine gearboxes. Wind Kraft Journal 2009;3:2–5.
[9] Muller J, Errichello R. Oil cleanliness in wind turbine gearboxes. Machinery lubrication, July.
[10] Mitchell F. Choosing the right wind turbine lubricant. Power engineering, April.
[11] Musial W, Butterfield S, McNiff B. Improving wind turbine gearbox reliability. In: European wind energy conference. Milan, Italy: National Renewable Energy Laboratory; May 7–10, 2007. p. 13.
[12] Doll GL. Tribological challenges in wind turbine technology. In: National renewable energy laboratory wind turbine tribology seminar; 2011.
[13] Evans RD. Classic bearing damage modes. In: National renewable energy laboratory wind turbine tribology seminar; 2011.
[14] Uyama H. The mechanism of white structure flaking in rolling bearings. In: National renewable energy laboratory wind turbine tribology seminar; 2011.
[15] Csoban A, Kozma M. Tooth friction loss in simple planetary gears. In: 7th international multidisciplinary conference. Baia Mare, Romania; May 17–18, 2007. p. 153–60.
[16] Hohn B-R, Michaelis K, Vollmer T. Thermal rating of gear drives: balance between power loss and heat dissipation. AGMA Technical Paper; 1996.
[17] Martins R, Cardoso N, Seabra J. Gear power loss performance of biodegradable low-toxicity ester-based oils. Proceedings of the Institution of Mechanical Engineers Part J—Journal of Engineering Tribology 2008;222(J3):431–40, http://dx.doi.org/10.1243/13506501jet345.
[18] Martins R, Seabra J, Brito A, Seyfert C, Luther A, Igartua R. Friction coefficient in FZG gears lubricated with industrial gear oils: biodegradable ester vs. mineral oil. Tribology International 2006;39(6):512–21, http://dx.doi.org/10.1016/j.triboint.2005.03.021.
[19] Martins R, Seabra J, Seyfert C, Luther R, Igartua A, Brito A. Power loss in FZG gears lubricated with industrial gear oils: biodegradable ester vs. mineral oil. In: Dowson MPGDD, Lubrecht AA, editors. Tribology and interface engineering series, vol. 48. Elsevier; 2005. p. 421–30.
[20] Martins R, Moura P, Seabra J. Power loss in FZG gears: mineral oil vs. biodegradable ester and carburized steel vs. austempered ductile iron vs. mos2-ti coated steel. VDI Berichte 1904.2 (1904 II); 2005. p. 1467–86.
[21] Magalhães L, Martins R, Locateli C, Seabra J. Influence of tooth profile and oil formulation on gear power loss. Tribology International 2010;43(10):1861–71 [36th Leeds-Lyon symposium special issue: multi-facets of tribology]. http://dx.doi.org/10.1016/j.triboint.2009.10.001.
[22] Eschmann P, Hasbargen L, Weigand K. Ball and roller bearings—theory, design, and application. John Wiley and Sons; 1985.
[23] SKF General Catalogue 6000 EN, SKF; November 2005.
[24] Linke H. Stirnradverzahnung. Hanser Verlag; 2010.
[25] Ariura Y, Ueno T. The lubricant churning loss and its behavior in gearbox in cylindrical gear systems. Journal of Japan Society of Lubrication Engineers 1975;20(3).
[26] Mauz W. Hydraulische Verlute von Stirnradgetrieben bei Umfangsgeschwindigkeiten bis 60 m/s (PhD thesis). Dissertation Uni Stuttgart; 1987.
[27] Maurer J. Ventilationsverluste. FVA Forschungsvorhaben Nr. 44/VI Heft 432; 1994:1–4.
[28] Changenet C, Velex P. A model for the prediction of churning losses in geared transmissions—preliminary results. Journal of Mechanical Design 2007;129 (1):128–33, http://dx.doi.org/10.1115/1.2403727.
[29] Changenet C, Leprince G, Ville F, Velex P. A note on flow regimes and churning loss modeling. Journal of Mechanical Design 2011;133(12):121009, http://dx.doi.org/10.1115/1.4005330.
[30] Csobán A, Kozma M. Influence of the oil churning, the bearing and the tooth friction losses on the efficiency of planetary gears. Journal of Mechanical Engineering 2010;56:245–52.
[31] Carlos MCG Fernandes, Pedro MP Amaro, Ramiro C Martins, Jorge HO Seabra. Torque loss in cylindrical roller thrust bearings lubricated with wind turbine gear oils at constant temperature. Tribol Int 2013;67:72–80. ISSN 0301-679X. http://dx.doi.org/10.1016/j.triboint.2013.06.016. ⟨http://www.sciencedirect.com/science/article/pii/S0301679X13002363⟩.
[32] Carlos MCG Fernandes, Ramiro C Martins, Jorge HO Seabra. Friction torque of cylindrical roller thrust bearings lubricated with wind turbine gear oils. Tribol Int 2013;59:121–128. ISSN 0301-679X. http://dx.doi.org/10.1016/j.triboint.2012.05.030. ⟨http://www.sciencedirect.com/science/article/pii/S0301679X12001922⟩.
[33] Fernandes CM, Martins RC, Seabra JH. Friction torque of thrust ball bearings lubricated with wind turbine gear oils. Tribology International 2013;58 (0):47–54, http://dx.doi.org/10.1016/j.triboint.2012.09.005 URL ⟨http://www.sciencedirect.com/science/article/pii/S0301679X12003015⟩.
[34] Carlos MCG Fernandes, Pedro MP Amaro, Ramiro C Martins, Jorge HO Seabra. Torque loss in thrust ball bearings lubricated with wind turbine gear oils at constant temperature. Tribol Int 2013;66:194–202, ISSN 0301-679X. http://dx.doi.org/10.1016/j.triboint.2013.05.002. ⟨http://www.sciencedirect.com/science/article/pii/S0301679X13002041⟩.
[35] Winter H, Michaelis K. FZG gear test rig—description and possibilities. In: Coordinate European council second international symposium on the performance evaluation of automotive fuels and lubricants; 1985.
[36] Hamrock BJ, Dowson D. Ball bearing lubrication. John Wiley & Sons; 1981 p. 386.
[37] Höhn B-R, Michaelis K, Hinterstoißer M. Optimization of gearbox efficiency. Goriva i Maziva 2009;48(4):462–80.
[38] Ohlendorf H. Verlustleistung und Erwärmung von Stirnrädern [Ph.D. thesis]. Dissertation TU München; 1958.
[39] Schlenk L. Unterscuchungen zur Fresstragfähigkeit von Grozahnrädern [Ph.D. thesis]. Dissertation TU München; 1994.